Kinetic modelling of the proton translocating CF_0CF_1-ATP synthase from spinach

Oliver Pänke, Bernd Rumberg*

Max-Volmer-Institut für Biophysikalische und Physikalische Chemie, Technische Universität, D-10623 Berlin, Germany

Abstract The rate of both ATP synthesis and hydrolysis catalysed by the thiol-modulated and activated ATP synthase from spinach is measured as a function of all substrates including the protons inside the thylakoid lumen. The most important findings are: (1) sigmoid kinetics with respect to H_{in}^+, (2) hyperbolic kinetics with respect to ADP, ATP and phosphate, with K_m for phosphate and ADP decreasing upon increasing H_{in}^+, (3) binding of ADP and phosphate in random order and competitive to ATP. Simulation of the complete set of experimental data is obtained by a kinetic model featuring Boyer's binding-change mechanism.

Key words: Chloroplast; ATP synthase; Photophosphorylation; Enzyme kinetics

1. Introduction

The ATP synthase of the F_0F_1-type reversibly catalyses the synthesis of ATP from ADP and inorganic phosphate. This key enzyme, which is found intrinsic to the membranes of chloroplasts, mitochondria and bacteria, uses the transmembrane proton gradient generated by electron transport as driving force for ATP synthesis (reviewed in [1–5]). The F_0 domain is totally membrane-embedded and involved in proton translocation while the F_1 domain is extrinsically attached and provided with a set of three catalytically active nucleotide binding sites which are located at the $\alpha\beta$-interfaces of the three circularly arranged $\alpha\beta$-subunits. The high-resolution structure for bovine heart F_1 obtained recently [6] has given strong support to the catalytic binding-change mechanism introduced by Boyer [7,8].

The ATP synthase from chloroplasts occurs embedded into the membrane of the thylakoid vesicles, the F_1 domain facing the outside aqueous phase. Due to light-induced vectorial electron transport the aqueous thylakoid lumen is loaded with protons whose backflow through the ATP synthase drives the synthesis of ATP. Reversal of this proton flow takes place if in the presence of excess ATP the hydrolysis of ATP is forced to occur. During steady-state conditions and with an ionic strength above 50 mM the proton-motive force controlling the ATP synthase consists of a transmembrane pH difference only, without the contribution of an electrical potential difference [9].

Here for the chloroplast CF_0CF_1-ATP synthase we present a thorough kinetic analysis of the steady-state reaction rate being varied by the concentrations of all substrates including the protons inside the thylakoid lumen. A straightforward reaction model is put forward which allows exact simulation of all experimental data. This model is essentially based on Boyer's hypothesis of cooperative binding-change. The main features are: (1) participation of three separate but interacting binding pockets on CF_1, each one passing sequentially through three different conformations from open over partially closed to strongly closed; (2) binding of ADP and phosphate in random order and competitive to ATP at the open pocket and spontaneous substrate conversion, $ADP + P \rightleftharpoons ATP + H_2O$, within the strongly closed pocket; (3) cooperative partial closing of the ligand-filled open pocket, strong closing of the partially closed pocket and opening of the strongly closed one induced by conformational changes released from the proton-driven events in CF_0; (4) translocation of four H^+ across CF_0 per ATP produced or hydrolysed; (5) overall rate-limiting quality of the release of ATP (or ADP during the reversed reaction cycle) from the open binding pocket. Preliminary results have been presented in [10].

2. Materials and methods

The experiments were performed with stirred suspensions of spinach thylakoids in a cylindrical reaction vessel (diameter 3 cm) at 20°C. The basic reaction medium contained in a volume of 6 ml 1 mM Tricine buffer, 50 mM KCl, 3 mM free $MgCl_2$, 15 µM pyocyanine, 3 µM thioredoxin, 500 µM dithiothreitol and chloroplasts equivalent to 10 µM chlorophyll. The starting pH was 8.00 and never changed by more than 0.05 units during each experiment, ensuring an unchanged buffer capacity. Loading of the thylakoid lumen with H^+ was initiated by illumination with red light through the vessel bottom. Different internal pH values could be achieved by changing the light intensity and/or the addition of different amounts of the proton permeability inducing agent nigericin combined with 500 nM valinomycin.

Each experiment was started by a preillumination for 90 s at maximal light intensity of 500 $W \cdot m^{-2}$. During this period, as a result of the influence of thioredoxin the ATP synthases are transferred into the reduced state. By this procedure the transmembrane ΔpH required for activation of the enzyme is forced down below ΔpH 2.0 [11]. Subsequently, the light intensity was adjusted for proper transmembrane ΔpH and ATP synthesis or ATP hydrolysis was started by addition of the nucleotide mixture. All experiments were performed under conditions of totally activated ATP synthases. This was achieved by taking care of a transmembrane ΔpH above 2.0, or, in the case of ATP hydrolysis as a function of H_{in}^+, by measuring the initial rate immediately after the end of the preillumination period.

The rates of synthesis or hydrolysis of ATP were obtained from the slope of the coupled pH changes in the medium according to [12]. Under the experimental conditions of pH 8.00, pMg 2.52, 0.07 M ionic strength and 20°C used here, exactly 0.94 H^+ are consumed per ATP formed [13]. The small pH changes were measured by a light-insensitive glass electrode with a flat membrane (SA 9218/2. N from Schott). The reference electrode (B 2830 from Schott) was separated from the reaction suspension by an electrolyte bridge filled with reaction medium.

The internal pH was obtained from the simultaneously monitored fluorescence quenching of added N-(1-naphthyl)ethylenediamine (NED) according to [14]. The wavelengths for excitation/detection

*Corresponding author. Fax (49) (30) 314-21122.
E-mail: rumberg@echo.chem.TU-Berlin.DE

of NED fluorescence were 351/434 nm and the light was guided by quartz fibres. A chopper frequency of 90 Hz was used for lock-in detection. The calibration with respect to pH_{in} was realized by a series of different equilibrium states at the ATP synthase where the phosphate potential is balanced by the transmembrane potential of H^+ as described in detail elsewhere [15,16]. The H^+/ATP coupling ratio of 4 used during this procedure has been confirmed recently [17]. The resulting calibration curve is presented in Fig. 1. Substrate-induced change of the internal pH was eliminated by application of the ΔpH-clamp technique where the internal pH is kept constant by continuous computer-controlled adjustment of the light intensity [18].

3 Results and discussion

3.1. Experimental steady-state kinetics of ATP synthesis and hydrolysis

We measured the rates of both ATP synthesis and hydrolysis catalysed by the thiol-modulated and activated ATP synthase of spinach chloroplasts as a function of the concentrations of ADP, ATP, phosphate and the protons located inside the thylakoids independent of each other. The results are presented in Figs. 2–4. The most important findings are: (1) sigmoid kinetics with respect to the internal proton concentration, H_{in}^+ (Figs. 2a, 3a); (2) hyperbolic Michaelis-Menten kinetics with respect to ADP, ATP and phosphate (Figs. 2b–d, 3b–d); (3) competition between ADP and ATP (Figs. 2c, 3c) as well as between phosphate and ATP (Figs. 2d, 3d); (4) for both phosphate and ADP a decrease of the Michaelis constant, K_m, along with the increase in maximal velocity, V_{max}, caused by enlargement of the transmembrane ΔpH (Fig. 4); (5) K_m values for ADP independent of phosphate and vice versa (results not shown).

3.2. Functional model of the ATP synthase used for simulation of the experimental results

The functional model introduced here is fundamentally based on the postulates of the cooperative binding-change mechanism which essentially may be described by three statements [4,5]. Firstly, the primary use of energy supplied by proton flow through F_0 is not to make ATP but rather to promote its release from tight binding sites at F_1 where it
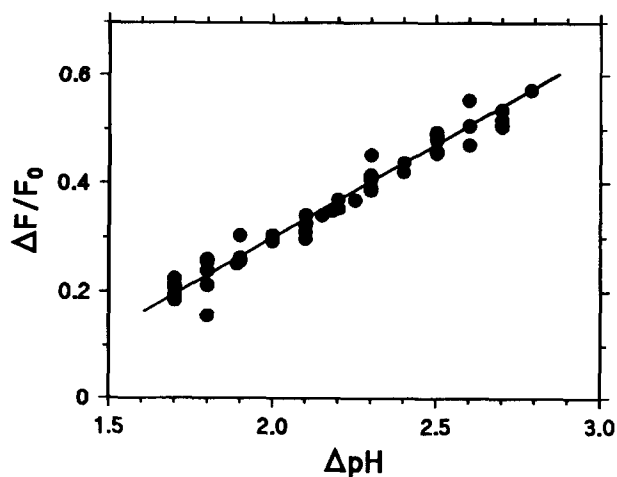
Fig. 1. Relationship between the relative decrease of NED fluorescence and the light-induced transmembrane ΔpH at pH 8.0 during steady-state conditions. ΔpH has been obtained from equilibrium states at the ATP synthase with implanted phosphate potentials, $\Delta G_P = \Delta G_P^0 + R \cdot T \cdot \ln([ATP]/([ADP] \cdot [P]))$, of different size according to the relation $\Delta pH = \Delta G_P/(2.303 \cdot n_P \cdot R \cdot T)$ using $\Delta G_P^0 = 32.1$ kJ mol^{-1} [13] and $n_P = 4$ [15,17].
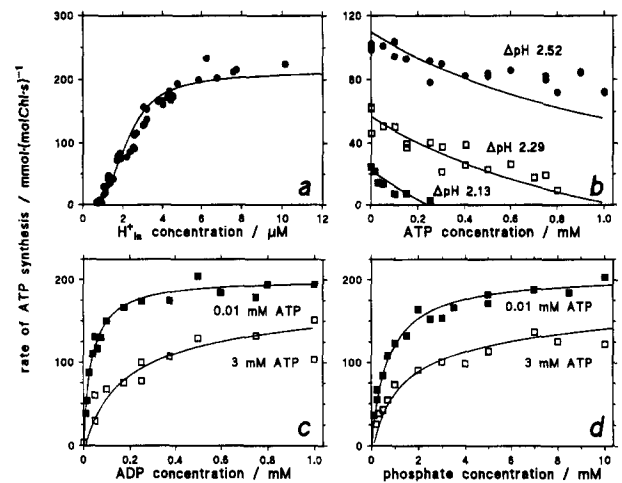
Fig. 2. Rate of ATP synthesis as a function of the concentrations of H_{in}^+, ATP, ADP and phosphate. (a) 1 mM phosphate, 1 mM ADP, 10 μM ATP, $E_0 = 1.30$ mmol·mol Chl^{-1}; (b) 1 mM phosphate, 300 μM ADP, $E_0 = 0.95$ mmol·mol Chl^{-1}; (c) ΔpH 2.54, 10 mM phosphate, $E_0 = 0.95$ mmol·mol Chl^{-1}; (d) ΔpH 2.55, 1 mM ADP, $E_0 = 0.95$ mmol·mol Chl^{-1}. The inserted curves have been calculated according to the reaction model presented in Fig. 5 and Table 1.

forms spontaneously. Secondly, during the catalytic cycle each binding site runs through three different states with increasing substrate affinity. The binding-changes occur simultaneously at three separate but interacting catalytic sites that remain 120° out of phase in the catalytic cycle. Thirdly, the transfer of energy between F_0 and F_1 is realized by the rotation of a shaft-forming aggregate of subunits relative to the rest of the enzyme. The detailed reaction pattern used here is presented in Fig. 5 and may be described as follows: (1) All three potent binding sites on F_1 are considered to participate equivalently in the catalytic reaction cycle. (2) Each binding site runs sequentially through three different conformations, named O (open site), L (loose site) and T (tight site), according to the nomenclature of Cross. The state O represents an open binding pocket where the product-substrate exchange with the aqueous medium takes place. The state T represents a closed pocket with tightly bound ligands. The process of substrate conversion, $ADP + P \rightleftharpoons ATP + H_2O$, is attributed to this state due to an intrinsic equilibrium constant near unity. The state L, due to its intermediate position between the states O and T, is arbitrarily characterized as a loosely closed binding pocket with intermediate substrate affinity. This state is supposed to be permanently occupied by ADP and phosphate during steady-state conditions. (3) After binding of ADP and phosphate at the O-site, loose closing (O → L), strong closing (L → T) and opening (T → O) occur simultaneously at all three interacting sites. (4) The binding changes in F_1 required for catalysis are postulated to be mechanically coupled to conformational changes which are released during proton translocation across F_0. This may be arranged by a rotation of subunits III and γ [19]. (5) Four protons must be translocated downhill across F_0 for each synthesized ATP molecule. This statement takes up the recent results on the H^+/ATP coupling ratio at this enzyme [15,17]. (6) The events attributed to the membrane-spanning F_0 domain are described as a series of four conformational changes $A_0 \rightarrow A_1 \rightarrow A_2 \rightarrow A_3 \rightarrow A_4$, each step being driven by the translocation of one proton across F_0 from the inside to the out-

side aqueous phase. This sequence of A-states may be visualized by the contraction of a spring. The regeneration step $A_4 \to A_0$ is supposed to be strictly coupled to the binding-change events occurring in F_1. (7) The principle of microreversibility is imposed on every single reaction step.

Mathematical handling is facilitated if fast equilibria are assumed for both the substrate conversion within the strongly closed binding pocket, $T:P \cdot ADP \rightleftharpoons T:ATP$, and the transitions between the A-states, $A_j + H_{in}^+ \rightleftharpoons A_{j+1} + H_{out}^+$ ($j = 0,1,2,3$). The corresponding equilibrium constants are denoted K_c and K_j, respectively. On the basis of the reaction sequence of O-states, namely $O:ATP \to O: \to O:ADP$ (alternatively $O:P) \to O:P.ADP \to O:ATP$ (see Fig. 5b), the five species of O-states are then calculable from a system of four linear independent steady-state equations and one balance equation. If it is assumed that ADP and phosphate bind independently of each other, this set of equations may be formulated as follows:

$$(k_{-ATP} + k_2) \cdot [O : ATP] - k_{ATP} \cdot [ATP] \cdot [O :] -$$
$$k_1 \cdot [O : P. ADP] = 0$$

$$(k_{ATP} \cdot [ATP] + k_P \cdot [P] + k_{ADP} \cdot [ADP]) \cdot [O :] -$$
$$k_{-ATP} \cdot [O : ATP] - k_{-P} \cdot [O : P] - k_{-ADP} \cdot [O : ADP] = 0$$

$$(k_P \cdot [P] + k_{-ADP}) \cdot [O : ADP] - k_{-P} \cdot [O : P.ADP] -$$
$$k_{-ADP} \cdot [ADP] \cdot [O :] = 0$$

$$(k_1 + k_{-ADP} + k_{-P}) \cdot [O : P. ADP] - k_P \cdot P \cdot [O : ADP] -$$
$$k_{ADP} \cdot [ADP] \cdot [O : P] - k_2 \cdot [O : ATP] = 0$$

$$[O :] + [O : ADP] + [O : P] + [O : P.ADP] + [O : ATP] = [E_0]$$

Subsequently, the overall reaction rate, v, may be calculated from:

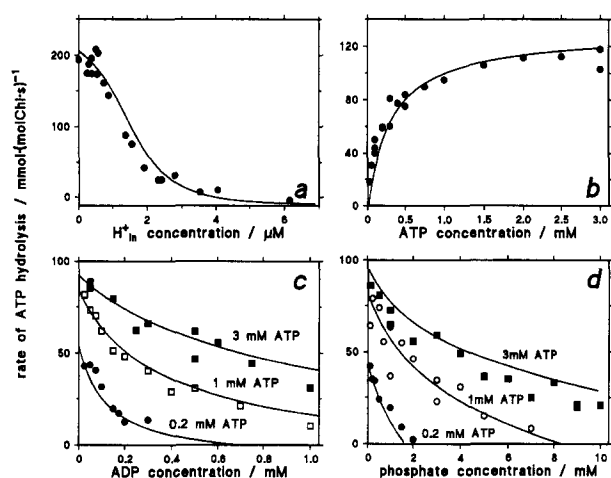$$v = k_{-ATP} \cdot [O : ATP] - k_{ATP} \cdot [ATP] \cdot [O :]$$

Fig. 3. Rate of ATP hydrolysis as a function of the concentrations of H_{in}^+, ATP, ADP and phosphate. (a) 1 mM phosphate, 50 µM ADP, 3 mM ATP, $E_0 = 0.95$ mmol·mol Chl^{-1}; (b) ΔpH 2.23, 100 µM phosphate, 50 µM ADP, $E_0 = 1.10$ mmol·mol Chl^{-1}; (c) ΔpH 2.27, 100 µM phosphate, $E_0 = 0.92$ mmol·mol Chl^{-1}; (d) ΔpH 2.25, 50 µM ADP, $E_0 = 0.92$ mmol·mol Chl^{-1}. The inserted curves have been calculated according to the reaction model presented in Fig. 5 and Table 1.
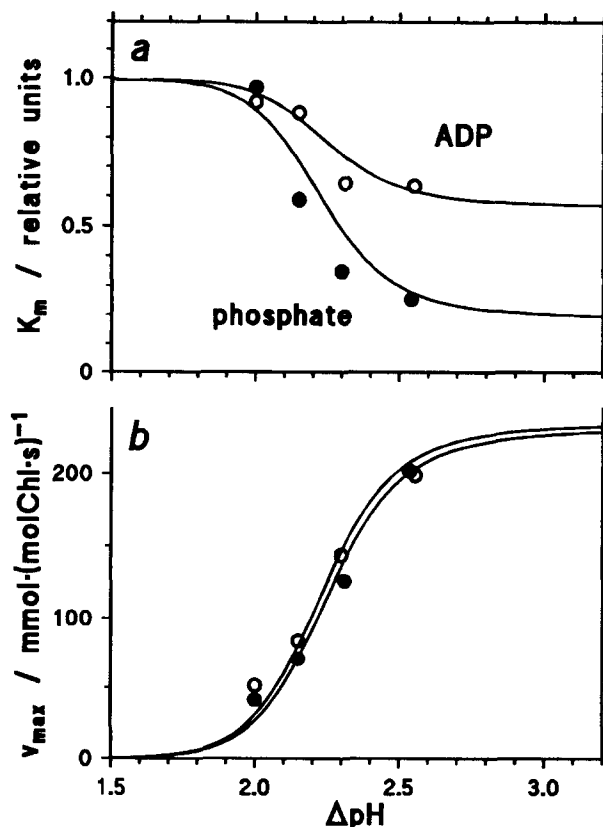

Fig. 4. Michaelis constants, K_m, of phosphate and ADP for stimulation of ATP synthesis (a) and accompanying maximal velocities, V_{max} (b), as a function of the transmembrane ΔpH. Cosubstrates were 1 mM ADP (●) or 10 mM phosphate (○). The inserted curves have been calculated according to the reaction model presented in Fig. 5 and Table 1. The starting K_m values correspond to 2.5 mM in the case of phosphate and 55 µM in the case of ADP.

An important specification should be added. The rate constants for the conformational changes in the direction of ATP synthesis and hydrolysis, k_1 and k_2, are burdened with probability factors, p_1 and p_2, according to the relations:

$$k_1 = k_1^\circ \cdot p_1 \text{ and } k_2 = k_2^\circ \cdot p_2$$

These probability factors take into account the simultaneous probabilities of the states T:ATP and A_4 for the forward and T:P.ADP and A_0 for the backward direction. For the sake of simplicity the four equilibrium constants K_j ($j=1,2,3,4$) are chosen identical. In that case these factors are given by:

$$p_1 = \frac{K_c}{1 + K_c} \cdot \frac{x^4}{D} \text{ and } p_2 = \frac{1}{1 + K_c} \cdot \frac{1}{D}$$

where

$$x = \frac{[H_{in}^+]}{[H_{out}^+]} \cdot \frac{1}{K} \text{ and } D = 1 + x + x^2 + x^3 + x^4.$$

The mathematical processing needed for the realization of the simulation concept was performed by numerical routine procedures on a standard PC. Optimal fit to the experimental data as shown in Figs. 2–4 is obtained if the equilibrium and rate constants listed in Table 1 are used. The total amount of enzyme, E_0, has been chosen between 0.9 and 1.3 mol·(mol Chl)$^{-1}$ fixed for each chloroplast preparation.

Table 1
Equilibrium and rate constants used for simulation of the experimental results

(a) Equilibrium constants
$K_c = 2.5$ [23]
$K_1 = K_2 = K_3 = K_4 = K = 220$

(b) Rate constants

$k_{ATP} = 2.08 \times 10^6 \ M^{-1}s^{-1}$	$k_{-ATP} = 2.70 \times 10^2 \ s^{-1}$	$(K_d = 130 \ \mu M)$
$k_{ADP} = 8.90 \times 10^6 \ M^{-1}s^{-1}$	$k_{-ADP} = 4.90 \times 10^2 \ s^{-1}$	$(K_d = 55 \ \mu M)$
$k_P = 8.10 \times 10^5 \ M^{-1}s^{-1}$	$k_{-P} = 2.03 \times 10^3 \ s^{-1}$	$(K_d = 2.5 \ mM)$
$k_1^0 = 5.13 \times 10^3 \ s^{-1}$	$k_2^g = 2.16 \times 10^3 \ s^{-1}$	

The resulting overall equilibrium constant for ATP synthesis amounts to $K_\Sigma = 2.4 \times 10^{-6} \ M^{-1}$. This corresponds to $\Delta G_1^\circ = 31.5 \ kJ \cdot mol^{-1}$ which is close to the value of $32.1 \ kJ \cdot mol^{-1}$, taken from [13] for the experimental conditions of pH 8.00, pMg 2.52, 0.07 M ionic strength and 20°C used here.

3.3. Concluding remarks

From the simulation analysis accomplished here it turns out that the maximal rates of ATP synthesis and hydrolysis are limited by the rates of release of ATP and ADP, respectively, from the O-site (see Table 1). This has not been taken into account in the binding-change model proposed previously [20], which is not qualified for simulation of the experimental data of Figs. 2–4. The characteristic feature of the reaction model presented here is the shift of the rate-limiting step for ATP synthesis from the binding-change step during conditions

of small transmembrane ΔpH to the step of release of ATP from the O-site during conditions of large ΔpH. This effect is caused by the ΔpH-induced acceleration of the binding-change. As a consequence the Michaelis constants, K_m, for phosphate and ADP are shifted downwards starting from the true dissociation constants, K_d, as shown in Fig. 4. This last result is at variance with the observations of Strotmann et al. [18]. These authors instead of the fluorescence quenching of NED used that of 9-aminoacridine (9-AA) for the control of the transmembrane ΔpH. Different from NED, 9-AA
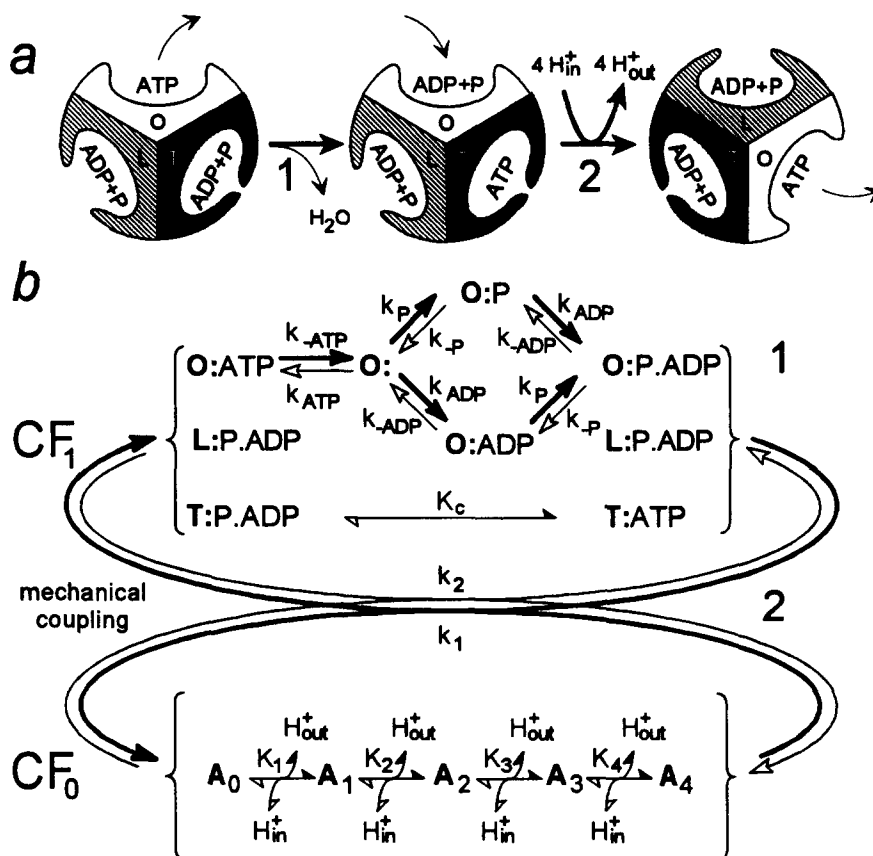

Fig. 5. (a) Modified version of Boyer's binding-change mechanism for ATP synthesis. The symbol O refers to the open state of the binding pocket allowing free substrate exchange with the aqueous medium. The symbols L and T refer to the loose and tight states which are permanently occupied by ligands. During step 1 product-substrate exchange at the open O-site and substrate conversion at the closed T-state occur simultaneously but independently of each other. During step 2 loose closing, strong closing and opening of the three binding sites occur in interacting fashion and strictly coupled to the conformational changes which are released from the proton-driven events in F_0. The entire catalytic cycle is complete in 3-fold repetition of reaction steps 1 and 2. (b) Detailed reaction pattern according to a. Solid arrows refer to synthesis of ATP and open arrows to hydrolysis. The symbols A_j ($j = 0,1,2,3,4$) refer to different conformational states of subunits not specified yet. Taking into account that during the entire catalytic reaction cycle three ATP molecules are synthesized or hydrolysed and 12 protons are translocated across F_0, it would appear that this is achieved by cooperation of 12 copies of subunit III in CF_0 (corresponding to subunit c in EF_0 from *E. coli*) whereby one proton is taken over by each copy and a rotary mechanism may be involved [4].

strongly interacts with nucleotide causing fluorescence quenching, the extent of which is influenced by transmembrane ΔpH and therefore interferes with light-induced fluorescence quenching. For this reason results obtained with 9-AA are questionable.

Finally, it should be emphasized that the satisfactory fit to the experimental data as shown in Figs. 2–4 has been obtained on the basis of a reaction model which only considers the minimal number of reaction steps and reaction constants. This proves the high degree of probability inherent in this model. However, the model does not allow one to distinguish whether three catalytic binding sites as outlined above or only two as suggested by Berden et al. [21,22] are involved in the catalytic reaction cycle. The set of linear equations remains unchanged if a cooperative bi-site reaction cycle is realized by omission of state L. In this case the mechanistical basis of the rotary hypothesis would be lost.

References

[1] Senior, A.E. (1990) Annu. Rev. Biophys. Chem. 19, 7–41.

[2] Fillingame, R.H. (1990) The Bacteria 12, 345–391.

[3] Nelson, N. (1992) Biochim. Biophys. Acta 1100, 109–124.

[4] Cross, R.L. (1992) in: Molecular Mechanism in Bioenergetics (Ernster, L. ed.) pp. 317–330, Elsevier, Amsterdam.

[5] Cross, R.L. (1994) Nature 370, 594–595.

[6] Abrahams, J.P., Leslie, A.G.W., Lutter, R. and Walker, J.E. (1994) Nature 370, 621–628.

[7] Boyer, P.D. (1989) FASEB J. 3, 2164–2178.

[8] Boyer, P.D. (1993) Biochem. Biophys. Acta 1140, 215–250.

[9] Huber, H.-L., Rumberg, B. and Siggel, U. (1980) Ber. Bunsenges. Phys. Chem. 84, 1050–1055.

[10] Pänke, O. and Rumberg, B. (1995) in: Photosynthesis: from Light to Biosphere, vol. III (Mathis, P. ed.) pp. 143–146, Kluwer, Dordrecht.

[11] Strelow, F. and Rumberg, B. (1993) FEBS Lett. 323, 19–22.

[12] Nishimura, M., Ito, T. and Chance, B. (1962) Biochim. Biophys. Acta 59, 177–182.

[13] Krab, K. and van Wezel, J. (1992) Biochim. Biophys. Acta 1098, 172–176.

[14] Schuldiner, S., Rottenberg, H. and Avron, M. (1972) Eur. J. Biochem. 25, 64–70.

[15] Rumberg, B., Schubert, K., Strelow, F. and Tran-Anh, T. (1990) in: Current Research in Photosynthesis, vol. III (Baltscheffsky, M. ed.) pp. 125–128, Kluwer, Dordrecht.

[16] Lohse, D., Thelen, R. and Strotmann, H. (1989) Biochim. Biophys. Acta 976, 85–93.

[17] Van Walraven, H.S., Strotmann, H., Schwarz, O. and Rumberg, B. (1996) FEBS Lett. (in press).

[18] Strotmann, H., Thelen, R., Müller, W. and Baum, W. (1990) Eur. J. Biochem. 193, 879–886.

[19] Duncan, T.M., Bulygin, V.V., Zhou, Y., Hutcheon, M.L. and Cross, R.L. (1995) Proc. Natl. Acad. Sci. USA 92, 10964–10968.

[20] Stein, W.D. and Läuger, P. (1990) Biophys. J. 57, 255–267.

[21] Berden, J.A., Hartog, A.F. and Edel, C.M. (1991) Biochim. Biophys. Acta 1057, 151–156.

[22] Edel, C.M., Hartog, A.F. and Berden, J.A. (1993) Biochim. Biophys. Acta 1142, 327–335.

[23] Fromme, P. and Gräber, P. (1990) Biochim. Biophys. Acta 1020, 187–194.